

PACS numbers: 12.38.Bx, 13.85.-t, 13.85.Hd

OBTAINING MATRIX ELEMENTS FOR 5-POINT ON-SHELL FEYNMAN DIAGRAMS

Z. Merebashvili

Institute of High Energy Physics, Iv. Javakhishvili Tbilisi State University, University Str. 9, 0109, Tbilisi, Georgia

Abstract. We obtain analytical results on the representation of the one-loop five-point on-shell amplitudes as a perturbative series up to $\mathcal{O}(\varepsilon^2)$ in the dimensional regularization parameter ε . These results are relevant for the next-to-next-to-leading-order (NNLO) quark-parton model description of the hadroproduction of heavy quarks. These one-loop matrix elements can also be used as input in the determination of the corresponding NNLO cross sections for heavy flavor photoproduction, and in photon-photon reactions.

Key words: Perturbative calculations, Hadron induced high- and super-high-energy interactions, Inelastic scattering.

I. Introduction

It has been already 25 years since the next-to-leading-order (NLO) corrections to the hadroproduction of heavy flavors were first presented in the seminal work [1]. These results were confirmed yet in another seminal work [2]. However, in all the NLO calculations there remains, among others, the problem that the renormalization and factorization scale dependences render the theoretical predictions to have much larger uncertainties than today's standards require. This calls for a next-to-next-to-leading-order (NNLO) calculation of heavy-quark production in hadronic collisions. In fact, the scale dependence of the theoretical prediction is expected to be considerably reduced when NNLO partonic amplitudes are folded with the available NNLO parton distributions.

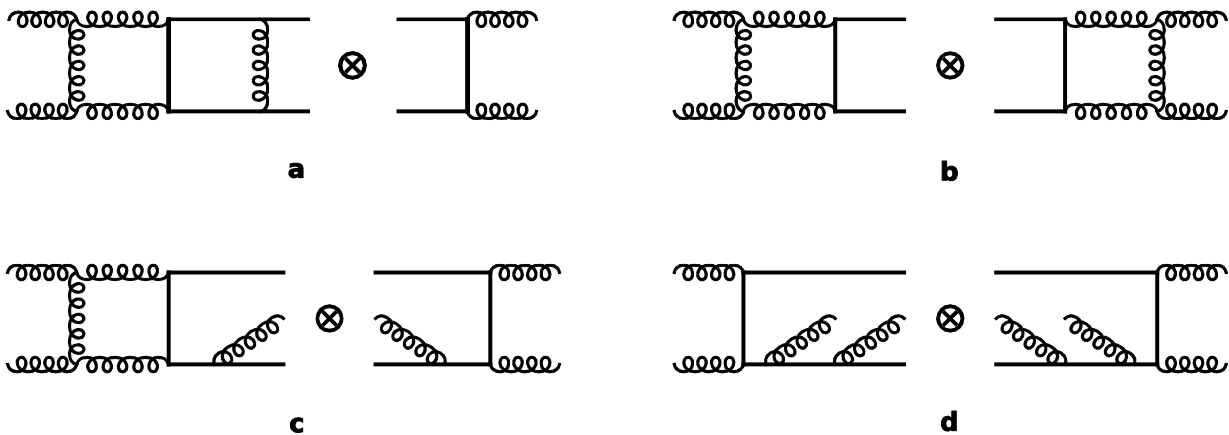


Fig. 1: Exemplary gluon fusion diagrams for the NNLO calculation of heavy-hadron production.

There are four classes of contributions that need to be calculated for the NNLO corrections to the hadronic production of heavy-quark pairs. In Fig. 1 we show one generic diagram each for the four classes of contributions that need to be calculated for the NNLO corrections to the gluon-initiated hadroproduction of heavy flavors. The first class involves the pure two-loop contribution

[1(a)], which has to be folded with the leading-order (LO) Born term. The second class of diagrams [1(b)] consists of the so-called one-loop squared contributions arising from the product of one-loop virtual matrix elements. Further, there are the one-loop gluon emission contributions [1(c)] that are folded with the one-gluon emission graphs. This is the topic of the present paper. Finally, there are the squared two-gluon emission contributions [1(d)] that are purely of tree type. The corresponding graphs for the quark-initiated processes are not displayed.

Bits and pieces of the NNLO calculation for hadroproduction of heavy flavors have been calculated in the recent years. In this context we would like to mention the two-loop calculation of the heavy-quark vertex form factor [3] that can be used as one of the many building blocks in the first class of processes. There is also a numerical approach applied to the calculation of the pure two-loop diagrams [4]. An analytic calculation of a subclass of the two-loop contributions to $q\bar{q} \rightarrow Q\bar{Q}$ was published [5]. The authors of Ref. [6] have calculated the NLO corrections to $t\bar{t}$ + jet production with contributions from the third class of diagrams. However, this result needs further subtraction terms in order to allow for an integration over the full phase space.

Regarding the second class of contributions, all the necessary master scalar integrals needed in this calculation have been assembled in Ref. [7], with the results expressed in terms of so-called L -functions, which can be written as one-dimensional integral representations involving products of log and dilog functions. Alternatively, in [8] the results for these scalar integrals are rewritten as a multitude of multiple polylogarithms of maximal weight and depth 4. The divergent and finite terms of the one-loop *amplitudes* for $q\bar{q} \rightarrow Q\bar{Q}$ and $gg \rightarrow Q\bar{Q}$ were given in Ref. [9]. The remaining $O(\varepsilon)$ and $O(\varepsilon^2)$ amplitudes have been written down in Ref. [10]. All these results were presented in a closed analytic form. The NNLO one-loop squared amplitudes for the quark-initiated process were presented in Ref. [11]. The calculation of the NNLO one-loop squared matrix elements for the process $gg \rightarrow Q\bar{Q}$ was done in [12], as well as in [13]. In Refs. [11, 12, 13] results for scalar master integrals of [7, 8] were used exclusively. The calculation is carried out in dimensional regularization [14] with space-time dimension $n = 4 - 2\varepsilon$. We mention that a closed-form, one-loop squared results for heavy-quark production in the fusion of real photons are presented in Ref. [15].

All the available results were collected and correspondingly combined in a semi-numerical calculation of the fully inclusive total cross section for top-quark production in Refs. [16, 17].

In our presentation, we shall make use of our notation for the coefficient functions of the relevant scalar one-loop master integrals calculated up to $O(\varepsilon^2)$ in Refs. [7, 8]. Taking the *complex* scalar three-point function C_i as an example, we define successive coefficient functions $C_i^{(j)}$ for the Laurent series expansion of C_i . One has

$$C_i = iC_\varepsilon(m^2) \left\{ \frac{1}{\varepsilon^2} C_i^{(-2)} + \frac{1}{\varepsilon} C_i^{(-1)} + C_i^{(0)} + \varepsilon C_i^{(1)} + \varepsilon^2 C_i^{(2)} + O(\varepsilon^3) \right\}, \quad (1)$$

where $C_\varepsilon(m^2)$ is defined by

$$C_\varepsilon(m^2) \equiv \frac{\Gamma(1+\varepsilon)}{(4\pi)^2} \left(\frac{4\pi\mu^2}{m^2} \right)^\varepsilon. \quad (2)$$

We use this notation for both the real and imaginary parts of C_i , i.e. for $\text{Re}C_i$ and $\text{Im}C_i$. Similar expansions hold for the arbitrary scalar one-, two-, three-, four- and five-point functions A_i, B_i, C_i, D_i , and E_i .

The aim of this work is to calculate the amplitudes that contribute to the 5-point graphs on the left-hand side of Fig. 1(c).

This paper is organized as follows. Section II contains an outline of our general approach, discusses renormalization procedures and normalization. Section III considers the single bremsstrahlung subprocesses that contribute to the hadroproduction of heavy flavours at NNLO as

shown in Fig. 1(c), as well as the relevant scalar integrals. In Sec. IV one finds a discussion of the calculation of the NNLO matrix elements for the gluon fusion subprocess. Our results are summarized in Sec. V.

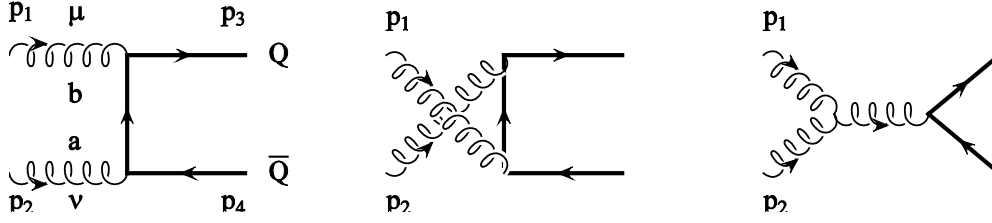


Fig. 2: The t -, u -, and s -channel LO graphs contributing to the gluon (curly lines) fusion amplitude. The thick solid lines correspond to the heavy quarks.

II. NOTATION

At the LO heavy-flavor hadroproduction proceeds through two partonic subprocesses: gluon fusion and light-quark-antiquark annihilation. The first subprocess is the most challenging one in QCD from a technical point of view. It has three production topologies already at the Born level (see Fig. 2). The second subprocess, where there is only one topology at the Born level, is depicted in Fig. 3. The one-gluon emission graphs that are to be folded with the one-loop $2 \rightarrow 3$ diagrams of class [1(c)] can be obtained from the graphs of Figs. 2 and 3 by insertion of an additional gluon external leg to every vertex, propagator and external line. The remaining tree $2 \rightarrow 3$ graphs arising at this $\mathcal{O}(\alpha_s^3)$ level of a QCD perturbation theory are due to a gluon-(light)quark annihilation (see Fig. 4) subprocess.

Irrespective of the partons involved, the general kinematics is, of course, the same in all these subprocesses. In general, we have

$$f(p_1) + f(p_2) \rightarrow Q(p_3) + \bar{Q}(p_4) + f(p_5), \quad (3)$$

where f stands for a light parton. The momentum flow directions correspond to the physical

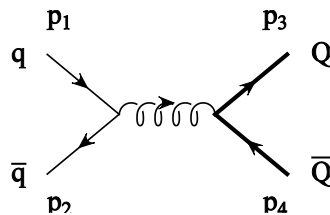


Fig. 3: The lowest order Feynman diagram representing light quark-antiquark annihilation. Normal solid lines represent the light quarks.

configuration, e.g. p_1 and p_2 are ingoing whereas p_3, p_4 and p_5 are outgoing. With m being the heavy-quark mass, we define

$$\begin{aligned} s &\equiv (p_1 + p_2)^2, & t &\equiv T - m^2 \equiv (p_1 - p_3)^2 - m^2, \\ u &\equiv U - m^2 \equiv (p_2 - p_3)^2 - m^2 \end{aligned} \quad (4)$$

and

$$s_2 \equiv S_2 - m^2 \equiv (p_1 + p_2 - p_3)^2 - m^2 = s + t + u. \quad (5)$$

Also

$$n = 4 - 2\varepsilon, \quad p_1 + p_2 = p_3 + p_4 + p_5, \\ p_1^2 = p_2^2 = p_5^2 = 0, \quad p_3^2 = p_4^2 = m^2.$$

We also introduce the overall factor

$$\mathbf{C} = \left(g_s^4 C_\varepsilon(m^2) \right)^2, \quad (6)$$

where g_s is the renormalized strong-coupling constant and $C_\varepsilon(m^2)$ is defined in Eq. (2).

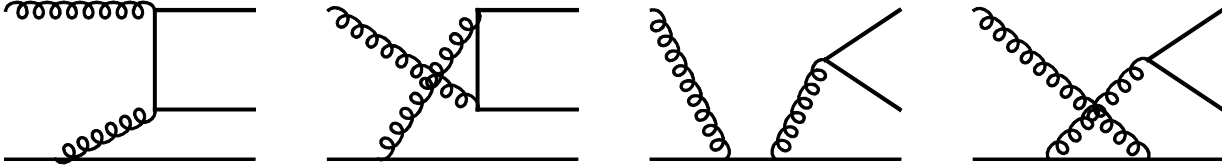


Fig. 4: The lowest order Feynman diagram representing light (anti)quark-gluon collision.

Our renormalization procedure is carried out in a mixed renormalization scheme. When dealing with massless quarks, we work in the modified minimal-subtraction ($\overline{\text{MS}}$) scheme, while heavy quarks are renormalized in the on-shell scheme defined by the following conditions for the renormalized external heavy-quark self-energy graphs:

$$\Sigma_r(p)|_{p=m} = 0, \quad \frac{\partial}{\partial p} \Sigma_r(p)|_{p=m} = 0. \quad (7)$$

In the on-shell scheme, the first condition in Eq. (7) ensures that the heavy-quark mass is the pole mass. For completeness, we list the set of one-loop renormalization constants used in this paper. One has

$$\begin{aligned} Z_1 &= 1 + \frac{g_s^2}{\varepsilon} \frac{2}{3} \left\{ (N_C - n_l) C_\varepsilon(\mu^2) - C_\varepsilon(m^2) \right\}, \\ Z_m &= 1 - g_s^2 C_F C_\varepsilon(m^2) \frac{3 - 2\varepsilon}{\varepsilon(1 - 2\varepsilon)}, \\ Z_2 &= Z_m, \\ Z_{1F} &= Z_2 - \frac{g_s^2}{\varepsilon} N_C C_\varepsilon(\mu^2), \\ Z_{1f} &= 1 - \frac{g_s^2}{\varepsilon} N_C C_\varepsilon(\mu^2), \\ Z_3 &= 1 + \frac{g_s^2}{\varepsilon} \left\{ \left(\frac{5}{3} N_C - \frac{2}{3} n_l \right) C_\varepsilon(\mu^2) - \frac{2}{3} C_\varepsilon(m^2) \right\} \\ &= 1 + \frac{g_s^2}{\varepsilon} \left\{ (\beta_0 - 2N_C) C_\varepsilon(\mu^2) - \frac{2}{3} C_\varepsilon(m^2) \right\}, \\ Z_g &= 1 - \frac{g_s^2}{\varepsilon} \left\{ \frac{\beta_0}{2} C_\varepsilon(\mu^2) - \frac{1}{3} C_\varepsilon(m^2) \right\}, \end{aligned} \quad (8)$$

with $\beta_0 = (11N_C - 2n_l)/3$ being the first coefficient of the QCD beta function, n_l the number of light quarks, $C_F = 4/3$, and $N_C = 3$ the number of colors. The arbitrary mass scale μ is the scale at which the renormalization is carried out. The above renormalization constants renormalize the

following quantities: Z_1 for the three-gluon vertex, Z_m for the heavy-quark mass, Z_2 for the heavy-quark wave function, Z_{1F} for the $(Q\bar{Q}g)$ vertex, Z_{1f} for the $(q\bar{q}g)$ vertex, Z_3 for the gluon wave function and Z_g for the strong-coupling constant α_s . For the massless quarks, there is no mass and wave function renormalization.

In order to fix our normalization, we write down the differential cross section for $gg \rightarrow Q\bar{Q}$ in terms of the squared amplitudes $|M|^2$. One has

$$d\sigma_{gg \rightarrow Q\bar{Q}} = \frac{1}{2s} \frac{d(\text{PS})_2}{4(1-\varepsilon)^2} \frac{1}{d_A^2} |M|_{gg \rightarrow Q\bar{Q}}^2, \quad (9)$$

where the n -dimensional two-body phase space is given by

$$d(\text{PS})_2 = \frac{m^{-2\varepsilon}}{8\pi s} \frac{(4\pi)^\varepsilon}{\Gamma(1-\varepsilon)} \left(\frac{tu - sm^2}{sm^2} \right)^{-\varepsilon} \delta(s+t+u) dt du. \quad (10)$$

We explicitly exhibit the flux factor $(4p_1 p_2)^{-1} = (2s)^{-1}$, and the spin $(n-2)^{-2} = (2-2\varepsilon)^{-2}$ and color d_A^{-2} averaging factors for the initial gluons. Here $d_A = N_C^2 - 1 = 8$ is the dimension of the adjoint representation of the color group $\text{SU}(N_C)$.

III Partonic subprocesses and master integrals

There are three topologically different partonic subprocesses that contribute to the hadron-hadron reaction at NNLO in perturbative QCD:

$$g + g \rightarrow Q\bar{Q} + g \quad (11)$$

$$q + \bar{q} \rightarrow Q\bar{Q} + g \quad (12)$$

$$g + q \rightarrow Q\bar{Q} + q \quad (13)$$

In the present article we study the production of heavy quark pairs in the gluon fusion subprocess (11). This is the most complicated subprocess as it contains graphs of many

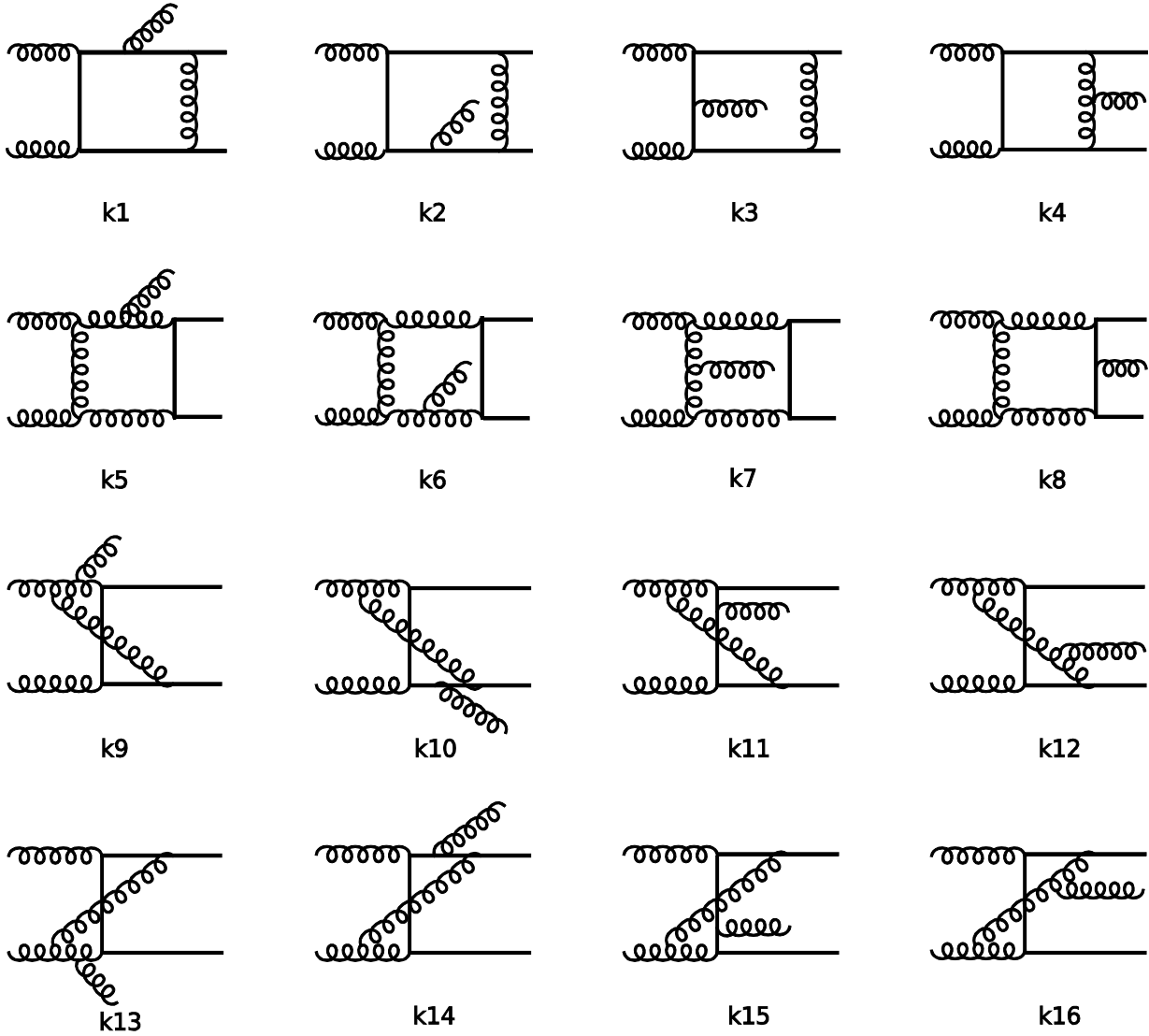


Fig. 5: The 5-point one-loop graphs contributing to the gluon fusion amplitude.

different topologies and hence allows the determination of the complete set of the master scalar integrals needed for the reduction of the 5-point integrals for the other two topologies as well.

In Fig. 5 we display the gluon fusion diagrams which contain the pentagon loops that produce the 5-point scalar integrals to be calculated. The one-loop five-point functions are defined by

$$E(q_1, q_2, q_3, q_4, m_1, m_2, m_3, m_4, m_5) = \quad (14)$$

$$\mu^{2\epsilon} \int \frac{d^n q}{(2\pi)^n} \frac{1}{(q^2 - m_1^2)[(q + q_1)^2 - m_2^2][(q + q_1 + q_2)^2 - m_3^2][(q + q_1 + q_2 + q_3)^2 - m_4^2][(q + q_1 + q_2 + q_3 + q_4)^2 - m_5^2]}.$$

The Feynman graphs to be calculated are shown in Fig. 5. The scalar 5-point integrals for the graphs k1-k4 are:

$$E_{k1}(p_4, -p_2, -p_1, p_5, 0, m, m, m, m); \quad (15)$$

$$E_{k2}(p_4, p_5, -p_2, -p_1, 0, m, m, m, m); \quad (16)$$

$$E_{k3}(p_4, -p_2, p_5, -p_1, 0, m, m, m, m); \quad (17)$$

$$E_{k4}(p_4, -p_2, -p_1, p_3, 0, m, m, m, 0); \quad (18)$$

There are only two independent scalar 5-point integrals out of the four above - E_{k3} and E_{k4} . The first two are obtained as follows:

$$E_{k1} = E_{k3}(p_1 \leftrightarrow -p_5), \quad E_{k2} = E_{k3}(p_2 \leftrightarrow -p_5). \quad (19)$$

Scalar integrals for the graphs k5-k8 can be obtained from the ones for k1-k4 above by the replacement $m \leftrightarrow 0$:

$$E_{k5}(p_4, -p_2, -p_1, p_5, m, 0, 0, 0, 0); \quad (20)$$

$$E_{k6}(p_4, p_5, -p_2, -p_1, m, 0, 0, 0, 0); \quad (21)$$

$$E_{k7}(p_4, -p_2, p_5, -p_1, m, 0, 0, 0, 0); \quad (22)$$

$$E_{k8}(p_4, -p_2, -p_1, p_3, m, 0, 0, 0, m); \quad (23)$$

Here there are also two independent scalar integrals E_{k7} and E_{k8} . The other two are obtained as

$$E_{k5} = E_{k7}(p_1 \leftrightarrow -p_5), \quad E_{k6} = E_{k7}(p_2 \leftrightarrow -p_5). \quad (24)$$

For the integrals corresponding to the diagrams k9-k12 one gets:

$$E_{k9}(p_4, -p_2, p_3, p_5, 0, m, m, 0, 0) = E_{k9}(-p_1, p_5, p_3, -p_2, 0, 0, 0, m, m); \quad (25)$$

$$E_{k10}(p_4, p_5, -p_2, p_3, 0, m, m, m, 0) = E_{k10}(-p_1, p_3, -p_2, p_5, 0, 0, m, m, m); \quad (26)$$

$$E_{k11}(p_4, -p_2, p_5, p_3, 0, m, m, m, 0) = E_{k11}(-p_1, p_3, p_5, -p_2, 0, 0, m, m, m); \quad (27)$$

$$E_{k12}(p_4, -p_2, p_3, -p_1, 0, m, m, 0, 0) = E_{k12}(-p_1, p_3, -p_2, p_4, 0, 0, m, m, 0), \quad (28)$$

where we have the relations

$$E_{k12} = E_{k9}(p_1 \leftrightarrow -p_5), \quad E_{k11} = E_{k10}(p_2 \leftrightarrow -p_5). \quad (29)$$

For the graphs k13-k16 one has to calculate the following scalar integrals:

$$E_{k13}(p_3, -p_1, p_4, p_5, 0, m, m, 0, 0) = E_{k13}(-p_2, p_5, p_4, -p_1, 0, 0, 0, m, m); \quad (30)$$

$$E_{k14}(p_3, p_5, -p_1, p_4, 0, m, m, m, 0) = E_{k14}(-p_2, p_4, -p_1, p_5, 0, 0, m, m, m); \quad (31)$$

$$E_{k15}(p_3, -p_1, p_5, p_4, 0, m, m, m, 0) = E_{k15}(-p_2, p_4, p_5, -p_1, 0, 0, m, m, m); \quad (32)$$

$$E_{k16}(p_3, -p_1, p_4, -p_2, 0, m, m, 0, 0) = E_{k16}(-p_2, p_4, -p_1, p_3, 0, 0, m, m, 0), \quad (33)$$

With

$$E_{k15} = E_{k14}(p_1 \leftrightarrow -p_5), \quad E_{k16} = E_{k13}(p_2 \leftrightarrow -p_5). \quad (34)$$

However, there are only two basic integrals out of the eight five-point functions relevant to the pentagon graphs k9-k16. These are E_{k9} and E_{k10} , and we have relations

$$E_{k13} = E_{k9}(p_4 \leftrightarrow p_3, p_2 \leftrightarrow p_1), \quad E_{k14} = E_{k10}(p_4 \leftrightarrow p_3, p_2 \leftrightarrow p_1). \quad (35)$$

Except for the t -channel pentagons depicted in Fig. 5, there are also the corresponding u -channel diagrams that can be obtained from the ones in Fig. 5 by $p_1 \leftrightarrow p_2$ interchange.

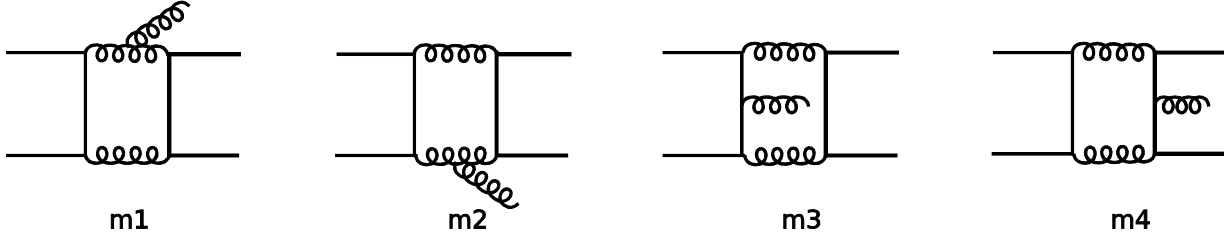


Fig. 6: The 5-point one-loop graphs contributing to the light quark-antiquark annihilation amplitude.

The Feynman diagrams for the subprocess (12) that generate 5-point functions are shown in Fig. 6. It is easy to see that these four graphs have exactly the same topology as the diagrams k5-k8 in Fig. 5. Therefore, for these scalar 5-point functions one has:

$$\begin{array}{cccc}
 \text{Diagram 11} & E_{m1} = E_{k5}, & E_{m2} = E_{k6}, & E_{m3} = E_{k7}, & E_{m4} = E_{k8}. \\
 \text{Diagram 12} & & & & \\
 \text{Diagram 13} & & & & \\
 \text{Diagram 14} & & & &
 \end{array} \quad (36)$$

Fig. 7: The 5-point one-loop graphs contributing to the gluon-light quark amplitude.

The eight relevant graphs for the subprocess (13) can be seen in Fig. 7. All four scalar 5-point integrals corresponding to these Feynman diagrams can be related to only one graph k5 of Fig. 3 as follows:

$$\begin{aligned}
 E_{11} &= E_{k5}(p_1 \rightarrow p_2, p_2 \rightarrow -p_5, p_5 \rightarrow -p_1), \\
 E_{12} &= E_{k5}(p_1 \rightarrow -p_5, p_5 \rightarrow -p_1), \\
 E_{13} &= E_{11}(p_3 \leftrightarrow p_4), \\
 E_{14} &= E_{12}(p_3 \leftrightarrow p_4).
 \end{aligned} \quad (37)$$

IV. Results

At LO for $gg \rightarrow Q\bar{Q}$, we shall use a representation which differs from the one given in Refs. [9, 10]. First note that there are only two independent color structures for this subprocess. The s -channel matrix element is a sum of two parts, each of which is proportional to one of the two independent color structures. We combine terms with the same color structures of the three (s , t , and u) production channels. Finally, we remove the heavy-antiquark momentum p_4 using energy-momentum conservation and use on-shell conditions for the gluons ($p_1 \cdot \varepsilon_1 = 0$ and $p_2 \cdot \varepsilon_2 = 0$) and the heavy quark ($\bar{u}_3 \cdot p_3 = \bar{u}_3 m$). We then obtain the two color-linked LO matrix elements

$$M_{LO,t} = iT^b T^a \hat{M}/t, \quad M_{LO,u} = iT^a T^b \hat{M}/u, \quad (38)$$

with

$$s\hat{M} = \gamma^\mu \not{p}_1 \gamma^\nu \not{s} + 2\gamma^\mu \not{p}_1^\nu \not{t} - 2\gamma^\nu \not{p}_2^\mu \not{t} - 2\gamma^\nu \not{p}_3^\mu \not{s} - 2 \not{p}_1 g^{\mu\nu} \not{t}. \quad (39)$$

It can be verified that the function \hat{M} is $t \leftrightarrow u$ symmetric, and consequently the color-linked Born amplitudes $M_{LO,t}$ and $M_{LO,u}$ turn into one another under $t \leftrightarrow u$.

We can then square the full Born matrix element $M_{LO,t} + M_{LO,u}$ and do the spin and color sums to obtain the LO amplitude,

$$|M|_{LO}^2 = \frac{d_A}{2} \left(C_F \frac{s^2}{tu} - N_C \right) |\hat{M}|^2 \equiv B, \quad (40)$$

where we have factored out a color-reduced Born term $|\hat{M}|^2$, which reads

$$|\hat{M}|^2 = 8 \left\{ \frac{t^2 + u^2}{s^2} + 4 \frac{m^2}{s} - 4 \frac{m^4}{tu} - \varepsilon 2 \left(1 - \frac{tu}{s^2} \right) + \varepsilon^2 \right\} \equiv \hat{B}. \quad (41)$$

The expression in Eq. (40) for the LO amplitude agrees with the well-known result in n dimensions (see e.g. Ref. [2]). Note that, by using the prescription of Ref. [18], we were able to avoid the introduction of ghost contributions which would otherwise arise from the square of the right-most three-gluon coupling amplitude in Fig. 2. In our case the prescription of Ref. [18] consists in the use of on-shell conditions for external gluons, i.e. $p_1 \cdot \varepsilon_1 = 0$ and $p_2 \cdot \varepsilon_2 = 0$, and the exclusion of the heavy-antiquark momentum via $p_4 = p_1 + p_2 - p_3$. When squaring amplitudes, we sum over the two helicities of the gluons using the Feynman gauge, i.e. we use

$$\sum_{\lambda=\pm 1} \varepsilon^\mu(\lambda) \varepsilon^\nu(\lambda) = -g^{\mu\nu}. \quad (42)$$

The use of the framework set up in Ref. [18] has the advantage in the non-Abelian case that one can omit ghost contributions when squaring the amplitudes. Using the above on-shell conditions already at the amplitude level means that one takes full advantage of the gauge invariance of the problem when squaring the amplitudes. Thus, in general, the results for the different channels will not be identical to the ones which would be obtained using 't Hooft-Feynman gauge throughout.

Due to the analysis done in the Section III it appears that we only need to obtain the required decomposition of the six independent 5-point scalar integrals in terms of a lower rank of basic universal set of scalar integrals. These scalar integrals to be determined are E_{k3} , E_{k4} , E_{k7} , E_{k8} , E_{k9} , and E_{k10} . All the other 5-point integrals needed for the hadroproduction of heavy quark pairs can be obtained via the use of the corresponding algebraic relations and/or relevant crossing. We have done the required decomposition of the above mentioned six master integrals in terms of the minimum number of on-shell and off-shell 1-, 2-, 3, and 4-point scalar integrals. We further folded the one-loop $2 \rightarrow 3$ amplitudes of the graphs of the topology depicted on the left-hand side of Fig. 1(c) with the relevant $2 \rightarrow 3$ tree amplitudes to obtain the squared matrix elements for the gluon fusion subprocess. The results are too long to be presented in the paper. In general, speaking of the $2 \rightarrow 3$ subprocesses, there are five independent scalar products fully describing its kinematics. However, we choose to express our matrix elements as combinations of scalar products of five partonic momenta $p_1 - p_5$. This is useful for two reasons. First, depending on the physical observable to be calculated, different parameterizations will be needed for the momenta. Second, when integrating over the three body phase space, partial fractioning needs to be performed; Having

all the five momenta explicitly present in the expressions is useful in avoiding appearance of many terms with spurious poles and thus useful in identifying true mass singularities. Computations in this work were done with the help of the REDUCE Computer Algebra System [19].

V. Conclusions

We have calculated analytically all the master scalar 5-point integrals which contribute to the one-loop squared matrix elements for heavy-quark pair production in the hadronic collisions. We have further squared the one-loop $2 \rightarrow 3$ amplitudes of the graphs of the topology depicted on the left-hand side of Fig. 1(c) with the matching $2 \rightarrow 3$ leading order tree partonic subprocesses to obtain the corresponding matrix elements contributing to various physical observables in the hadroproduction of heavy quarks at NNLO. Our results form part of the NNLO description of heavy-quark pair production relevant for the NNLO analysis of ongoing experiments at the LHC.

Acknowledgments

The work of Z.M. was supported by the Georgian Shota Rustaveli National Science Foundation through Grant No. FR 11/24.

References

1. P. Nason, S. Dawson, and R. K. Ellis, Nucl. Phys. (1988), **B303**, 607; Nucl. Phys. (1989) **B327**, 49 ; (1990) **B335**, 260(E).
2. W. Beenakker, H. Kuijf, W. L. van Neerven, and J. Smith, Phys. Rev. (1989) D **40**, 54; W. Beenakker, W. L. van Neerven, R. Meng, G. A. Schuler and J. Smith, Nucl. Phys. (1991) **B351**, 507.
3. W. Bernreuther, R. Bonciani, T. Gehrmann, R. Heinesch, T. Leineweber, P. Mastrolia, and E. Remiddi, Nucl. Phys. (2005) **B706**, 245.
4. M. Czakon, Phys. Lett. (2008) B **664**, 307.
5. R. Bonciani, A. Ferroglia, T. Gehrmann, D. Maître and C. Studerus, J. High Energy Phys. (2008) 07 129.
6. S. Dittmaier, P. Uwer, and S. Weinzierl, Phys. Rev. Lett. (2007), **98**, 262002.
7. J.G. Körner, Z. Merebashvili, and M. Rogal, Phys. Rev. (2005), D **71**, 054028.
8. J.G. Körner, Z. Merebashvili and M. Rogal, J. Math. Phys. (2006), **47**, 072302.
9. J. G. Körner and Z. Merebashvili, Phys. Rev. (2002), D **66**, 054023.
10. J.G. Körner, Z. Merebashvili, and M. Rogal, Phys. Rev. (2006), D **73**, 034030.
11. J.G. Körner, Z. Merebashvili, and M. Rogal, Phys. Rev. (2008), D **77**, 094011.
12. B.A. Kniehl, J.G. Körner, Z. Merebashvili, and M. Rogal, Phys. Rev. (2008), D **78**, 094013.
13. C. Anastasiou and S. Mert Aybat, arXiv:0809.1355 [hep-ph].
14. C.G. Bollini and J.J. Giambiagi, Phys. Lett. (1972), **40B**, 566; G. 't Hooft and M. Veltman, Nucl. Phys. (1972), **B44**, 189; J.F. Ashmore, Lett. Nuovo Cimento (1972), **4**, 289.
15. J.G. Körner, Z. Merebashvili, and M. Rogal, Phys. Rev. (2006), D **74**, 094006.
16. M. Czakon, P. Fiedler, and A. Mitov, Phys. Rev. Lett. (2013), **110**, 252004.
17. M. Czakon, M.L. Mangano, A. Mitov and J. Rojo, (2013) , JHEP 1307 167.
18. W.C. Kuo, D. Slaven, and B.L. Young, Phys. Rev. (1988), D **37**, 233.
19. A. Hearn, *REDUCE User's Manual Free Version* (2012).

Article received: 2015-02-21